Rare Metal Materials and Engineering
Volume 49, Issue 5, May 2020
Available online at www.rmme.ac.cn

Science Press

Cite this article as: Rare Metal Materials and Engineering, 2020, 49(5): 1546-1552.

ARTICLE

Microstructure and Properties of WC-based Coating Reinforced by Fe-based Amorphous Alloys

Xu Liping, Song Jinbing, Deng Changguang, Liu Min, Zhou Kesong

The Key Lab of Guangdong for Modern Surface Engineering Technology, National Engineering Laboratory for Modern Materials Surface Engineering Technology, Guangdong Institute of New Materials, Guangzhou 510651, China

Abstract: WC-CoCr/35wt% amorphous Fe-based alloy composite coating has been prepared by high velocity oxygen fuel (HVOF) spraying. Microstructure, hardness, wear resistance, high temperature oxidation and corrosion resistance of the composite coating were comparatively studied with WC-CoCr coating. XRD analysis and SEM observation show that the composite coating is mainly composed of WC, W_2C and a Fe-based amorphous phase. In comparison with WC-CoCr coating, the hardness of the composite coating is slightly decreased, but there is no statistically significant difference between them. As a result of hardness decrease, the wear resistance of the composite coating is a little bit inferior to that of the WC-CoCr coating. Results of high temperature oxidation at 800 ^{o}C prove that the composite coating exhibits excellent thermal stability, which is mainly attributed to the formation of a dense and uniform oxide layer during the high temperature oxidation test. Moreover, electrochemical test reveals that the corrosion resistance of the composite coating is better than that of WC-CoCr coating in 3.5wt% NaCl solution.

Key words: WC-based coating; amorphous; HVOF; wear resistance; corrosion resistance

High velocity oxy-fuel (HVOF) sprayed WC based cermet such as WC-Co, WC-CoCr and WC-Ni have found wide application in many industries due to their excellent wear resistance[1-4]. In the coatings, the hard WC particles lead to high coating hardness and high wear resistance, while the metal binder (Co, Ni or Co-Cr) supplies the necessary coating toughness[5-7]. The mechanical properties of cermets are related to the size and distribution of ceramic particles, as well as the content and composition of the metal binder phase. It is worth mentioning that simultaneous hardening and toughening effects were found for WC-(nano WC-Co) with micro WC strengthening particles in nano WC-Co cermet matrix[8]. And investigation on cold-sprayed coating using the WC-(nano WC-Co) cermet powder showed that the coating exhibited much higher hardness and toughness and thereby much higher wear resistance than HVOF-sprayed WC-Co coating with micro-sized WC particles[9]. However, with the price increase of W, Co, Ni, the costs of both WC based cermet powder and coatings also increase. Moreover, thermal stability becomes more and more crucial for the development of the coatings, as many applications involve long-term high temperature exposure[10]. Although Cr_3C_2-NiCr coating is used for protection of materials from high-temperature wear and erosion[11], its wear resistance is less than that of WC-based cermet[12]. Nevertheless, most of WC-based coatings cannot be used at the temperature over 500 °C. Meanwhile, the weight of the WC coating is relatively high owing to its high density. Therefore, the high weight, high price and limited thermal stability restrict the further application of WC based coatings.

A potential solution is to apply a composite coating consisting of Fe-based amorphous alloy in a WC based cermet matrix. By this way, it is possible to utilize the low friction

Received date: June 25, 2019
Foundation item: Science and Technology Planning Project of Guangdong Province (2017A070701027); Science and Technology Planning Project of Guangzhou (201707010455); National Natural Science Foundation of China (51771059); Natural Science Foundation of Guangdong Province (2016A030312015); GDAS's Project of Science and Technology Development (2017GDASCX-0202, 2018GDASCX-0402)
Corresponding author: Xu Liping, Ph. D., Senior Engineer, Guangdong Institute of New Materials, Guangzhou 510651, P. R. China, Tel: 0086-20-61086656, E-mail: xuliping@gdinm.com

coefficient[13], high corrosion resistance[14,15], good ability to resist high temperature[16], lower weight and lower price of the Fe-based amorphous alloy along with the superior abrasion resistance of the WC based cermet. In addition, research on Fe-based amorphous composite coating with WC-based cermet as reinforcement phase showed that HVOF is appropriate to prepare the composite coatings containing Fe-based amorphous alloys and WC-based cermet[14,17,18]. It is also reported that the deposition efficiency of WC based powders in the HVOF process is about 45%, while the deposition efficiency of mixture WC and amorphous powder in HVOF process can reach up to 57%[19]. Furthermore, it is reported that the addition $Fe_{42.87}Cr_{15.98}Mo_{16.33}C_{15.94}B_{8.88}$ (at%) in WC-10Co-4Cr coating at a powder mass ratio of 1:3 improved the corrosion resistance of WC coating, but there is no improvement in the wear resistance of the composite coating compared with the WC coatings[20]. However, investigation on WC-based coatings with Fe-based amorphous alloys as additional/reinforcement phase are still scarce. Also, there is no report on the comprehensive influence of Fe-based amorphous alloys on WC-based cermet coatings. Therefore, in the present work, the microstructure, wear resistance, high temperature oxidation resistance and corrosion resistance of HVOF sprayed WC-CoCr/FeCrMoWBMnCSi amorphous alloy composite coatings and pure WC-CoCr coatings were comparatively investigated to illuminate the effect of the addition of Fe-based amorphous alloy on the WC-CoCr coating.

1 Experiment

A commercially available WC-10wt%Co-4wt%Cr agglomerated and sintered powder with a nominal size distribution of 10~38 μm was obtained from GTV GmbH. A commercial Fe based amorphous powder (SHS7170) with a nominal size range of 15~53 μm was obtained from Nanosteel Company Inc. The nominal alloy composition was 20%Cr, 10%W, 5%B, 5%Mn, 5%Mo, 2%C, 2%Si (all in wt%) with the balance being Fe. WC-CoCr and Fe-based amorphous powders with the mass ratio of 65:35 were homogeneously mixed before spraying. The SEM images of precursor powder particles are shown in Fig. 1. A commercial HVOF spraying system (GTV HVOF K2, GTV Verschleißschutz, Germany) was used for thermal spraying of the WC-CoCr power and the mixed powder. The coating was deposited onto 304 stainless steel substrate with a dimension of 30 mm×50 mm×4 mm. Before spraying, the substrates were degreased with acetone and then grit blasted to get a rough surface. The used process parameters are listed in Table 1.

Cross sectional microstructures of the as-sprayed coatings were examined on a scanning electronic microscope (SEM, Nova nano 450) coupled with an energy-dispersive X-ray system (EDS). The phase composition of the coating was identified by an X-ray diffractometer (XRD, D/MAX -IIIA, Riguka).

The hardness of the as-sprayed coatings was evaluated using a MH-5 microhardness tester with a 300 g load applied for 15 s. The reported value is an average of ten different measurements, which were performed on different cross-section locations of the coatings.

The coated samples with a dimension of 50 mm×30 mm×4 mm were used for wear testing. A piece of SiC abrasive paper with grit size F180 was used as the counter material under the load of 30 N. The test was repeated for 2000 strokes. Before and after every 400 strokes, the mass of the test samples was measured using a high precision digital weight balance with 0.1 mg accuracy. Wear resistance was evaluated by the weight loss.

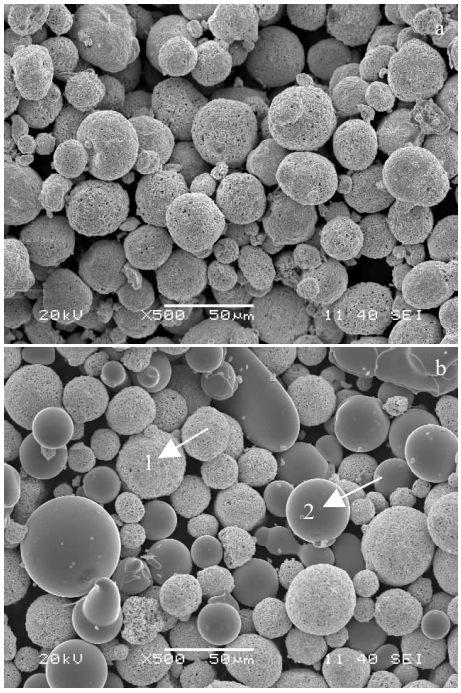

Fig.1 SEM images of the precursor powder particles: (a) WC-CoCr and (b) mixture of WC-CoCr and Fe-based metallic glass (1-WC-CoCr particle; 2-Fe-based metallic amorphous particle)

Table 1 HVOF parameters for as-sprayed coatings

Parameter	Value
Oxygen/L·min^{-1}	900
Kerosene/L·min^{-1}	26
Spray distance/mm	380
Transverse speed/mm·s^{-1}	1000
Powder feed rate/g·min^{-1}	100 (WC-CoCr powder)
	70 (mixed powder)

The coated samples with a dimension of 10 mm×12 mm×4 mm were put into a muffle furnace which has been preheated to 800 °C. After that, the furnace was opened for air exchange and then closed every 30 min. After heating at 800 °C for 2 h, the samples were cooled down to room temperature in the furnace and then taken out for observation and analysis.

The thermal behaviors of Fe-based amorphous alloy powder were detected from 200 °C to 900 °C at a rate of 5 °C/min by a Netzsch STA 449C differential scanning calorimeter in a nitrogen atmosphere and an air atmosphere, respectively.

Corrosion behavior was investigated by potentiodynamic polarization tests. Before testing, the specimens were mechanically polished, then cleaned in ethanol and dried in air. Potentiodynamic polarization measurements were performed with a potentiostat (PARSTAT 4000) in a standard three-electrode system with a platinum sheet as the counter electrode, a saturated calomel electrode (SCE) as the reference electrode and the coating specimen as the working electrode. The samples were polarized from -400 mV (vs. OCP) to 1300 mV (vs. OCP) at a potential scanning rate of 0.5 mV/s in a 3.5 wt% NaCl solution after the open circuit potential (OCP) became almost steady.

A *t* test was used to determine whether any significant differences existed between the mean values of hardness of the composite coating and the WC-CoCr coating. A difference between the two kinds of coatings was considered to be significant at $p < 0.05$.

2 Results and Discussion

2.1 Microstructure and phase composition

Fig.2 exhibits the cross-sectional microstructure and the EDS results of the as-sprayed coatings. It can be seen that the WC-CoCr coating shows a relatively dense layer structure (Fig.2a), and is mainly composed of W, Co, and Cr as shown in Fig.2b. The composite coating also shows a comparatively compact lamellar structure with bright and dark areas, which is attributed to the high atomic number of W. EDS analysis on bright area exhibits a similar result in WC-CoCr coating, validating that the bright area is WC-CoCr, while the dark area is inferred to be amorphous Fe-based alloy, as shown in Fig.2d. The volume fraction of Fe-based alloy is about 49%.

Fig.3 displays XRD patterns of the original powders of WC-CoCr and amorphous Fe-based alloy and of the as-sprayed coatings. The WC-CoCr powder is mostly WC phase and a small amount of W_2C phase and of unalloyed β-Co phase. The amorphous Fe-based powder shows the typical broad diffraction peaks of amorphous materials. The WC-CoCr coating contains more W_2C phase than that in the original powder owing to the presence of WC decomposition in high temperature and oxidizing conditions[21]. The diffraction peaks of β-Co phase disappear and no α-Co phase is detected in the WC-CoCr coating, indicating reactions between WC and Co[10] rather than a phase transformation from β-Co to α-Co[9]. The diffraction peaks of the composite coating are similar to those of WC-CoCr coating, and weak diffraction signal of amorphous phase is detected between 40°~45°. Combined the EDS results, it can be confirmed that the dark area in the composite coating is Fe-based amorphous alloy.

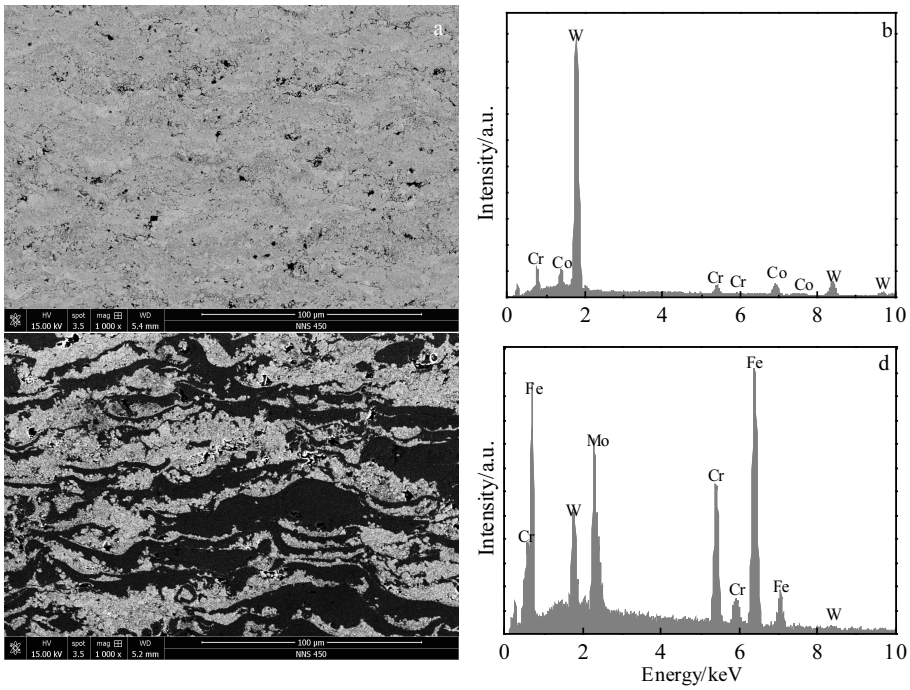

Fig.2 Cross sectional morphology (a, c) and EDS analysis (b, d) of WC-CoCr coating (a, b) and composite coating (c, d)

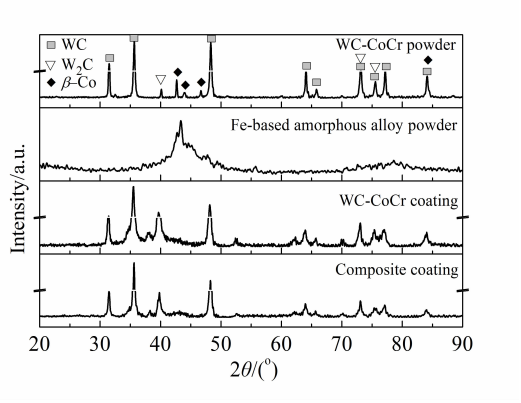

Fig.3 XRD patterns of WC-CoCr powder, Fe-based metallic alloy powder, HVOF WC-CoCr coating and HVOF composite coating

2.2 Hardness and wear resistance

The microhardness values of the as-sprayed coatings are listed in Fig.4. The results indicate that the microhardness ($HV_{0.3}$) of WC-CoCr coating is 11 710 MPa, while that of the composite coating is 10 260 MPa. After adding the amorphous Fe-based alloy, the microhardness of the coating is decreased by about 150, but no obvious statistically significant difference emerges between the two kinds of coatings (p>0.05). It was also reported that the surface hardness of WC-12Co cermet and Fe-based amorphous alloy composite coating was not considerably affected by the WC-12Co fraction[17].

Fig.5 shows the abrasion test results of the coatings. For both the WC-CoCr and the composite coatings, the wear loss increases in proportion to the numbers of reciprocating strokes (wear distance). The mass loss of the WC-CoCr coating is less than that of the composite coating during the test, suggesting the WC-CoCr coating exhibits better wear resistance. As is well-known, there is an inverse correlation between surface hardness and wear loss when surfaces come into contact with each other causing friction and wear[22.23]. So the better wear resistance of WC-CoCr coating may be attributed to its slightly higher surface hardness. In addition, some work reveals that the addition of hard phases can well improve the wear properties of alloys and metal-matrix composites[24,25]. Accordingly, it might be deduced that the addition of soft phase (amorphous Fe-based alloy) decreases the wear properties of the WC-CoCr matrix composite to some degree.

Fig.6 exhibits the micro morphology of the coatings after the abrasion test. A large amount of grooves caused by abrasive wear and pits formed by partial peeling off can be observed on both the WC-CoCr coating and the composite coating. The grooves on the WC-CoCr coating are less deeper as compared with those in the composite coating. It has been reported that wear tracks were formed because of the plastic flow resulting from the yielding and extrusion of CoCr binder, and penetration of the abrasive particles depends on the hardness of the material[4]. Therefore, based on the abrasion test results as shown in Fig.5 and Fig.6, it can be concluded that the addition of the Fe-based amorphous alloy decreases the hardness to some extent and thus the wear resistance of the composite coating is inferior to that of the WC-CoCr coating.

2.3 High temperature oxidation properties

Fig.7 shows the micro morphology of the coatings after the high temperature oxidation test. It can be found that the WC-CoCr coating is oxidized, and the oxidation coating is peeled off, while the composite coating exhibits an intact and dense morphology without any obvious peeling.

Fig.8 presents the surface microstructure, cross-sectional microstructure and element distribution maps of the composite coating after high temperature oxidation test. As can be seen, the surface is relatively dense with some small cracks (Fig.8a). From the cross-sectional morphology, it can be found that there is a reaction layer on the top of the composite coating, as shown in Fig.8b. Element distribution maps (Fig.8c~8j) on the cross section reveal that the reaction layer contains O, W, Co, Cr, Fe, Mn and a small amount of C and Mo, while the coating mainly contains W, Co, Cr, Fe, Mn and Mo, implying that the reaction layer consists mainly of oxide.

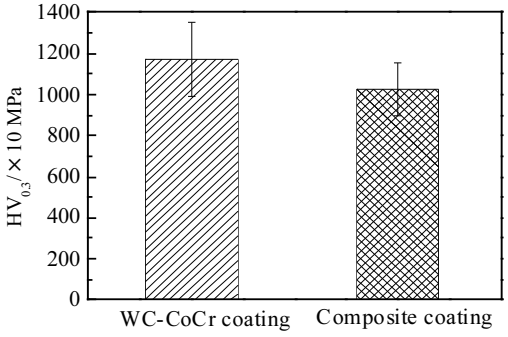

Fig.4 Vickers hardness of WC-CoCr coating and composite coating after thermal test (p>0.05)

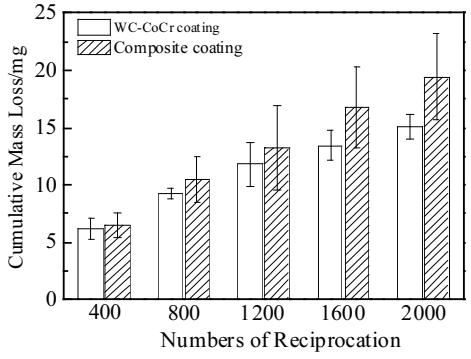

Fig.5 Mass loss of WC-CoCr coating and composite coating during abrasion test

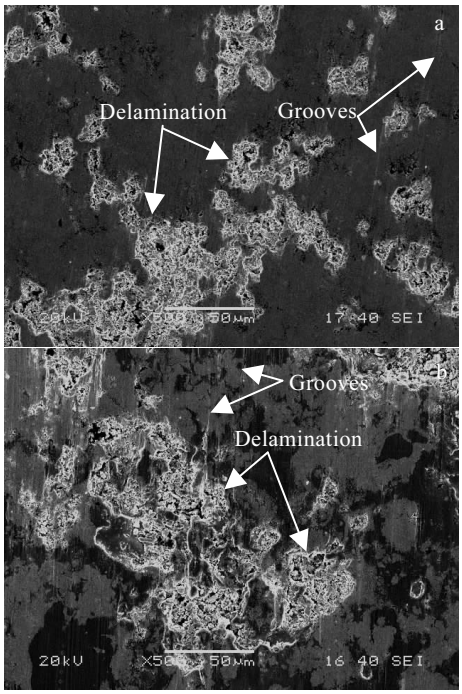

Fig.6 SEM micrographs of wear worn surfaces of WC-CoCr coating (a) and composite coating (b)

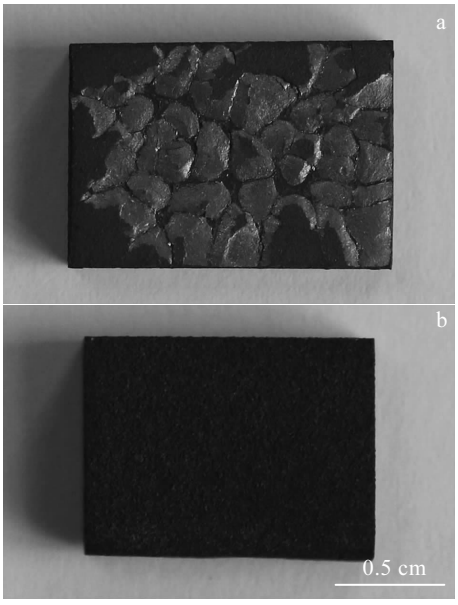

Fig.7 Macro morphologies of WC-CoCr coating (a) and composite coating (b) after high temperature oxidation test

Fig.9 shows XRD patterns of the coatings after high temperature oxidation test. Besides WC and W_2C detected on the as-sprayed coating, WO_3, $CoWO_4$ and other oxides are detected on the WC-CoCr coating. By contrast, only $CoWO_4$ phase and a tiny amount of Cr-W-O phase are detected on the composite coating.

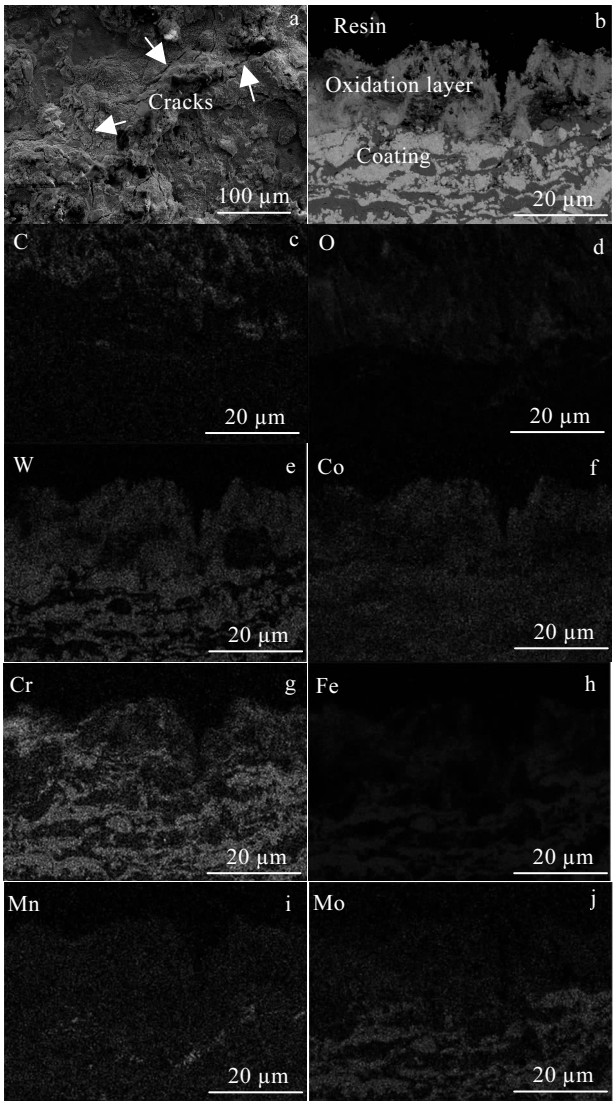

Fig.8 Surface micro morphology (a), cross-sectional micro morphology (b) and element distribution maps (c~j) of the composite coating after thermal treatment test

In order to further clarify the high temperature oxidation of the composite coating, DSC traces of Fe-based amorphous alloy powder were examined, as shown in Fig. 10. From the DSC curves in N_2 atmosphere, three exothermic peaks with peak temperatures of 622, 678 and 783 °C, are observed with an onset crystallization temperature (T_x) of 602 °C. Based on the DSC curves in air atmosphere, five exothermic peaks are found with a T_x of 604 °C. The peak temperatures of the first three exothermic peaks are 623, 679 and 786 °C, respectively, which are close to the peak temperatures of the three exothermic peaks detected in N_2 atmosphere, indicating that the first three peaks correspond to the crystallization process, and the latter two exothermic peaks are related to oxidation process. Combined with

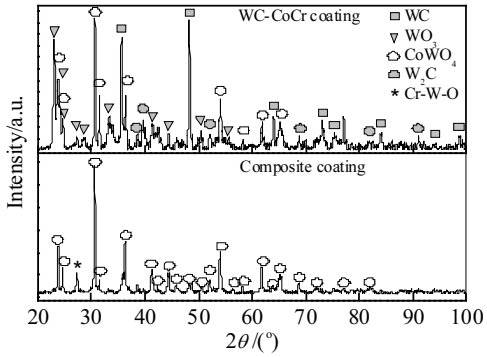

Fig.9 XRD patterns of WC-CoCr coating and composite coating after high temperature oxidation test

the micro structure, element distribution mapping and XRD results, it can be deduced that Fe-based amorphous alloy in the composite is also oxidized to some extent, but the amount of oxidation product is too tiny to be detected by XRD.

Research on HVOF WC-Co coatings found that formation of the surface oxide layer inhibits further oxidation of the deeper layer of the coating at 650 °C[26], but the WO_3 and $CoWO_4$-based oxide scale is not protective at temperatures around 800 °C[27]. In this case, both the WC-CoCr coating and the composite coating are oxidized during the high temperature oxidation test. The surface oxide layer of the WC-CoCr coating is partially peeled off and thus it is hard to prevent further oxidation, which is similar to the findings reported in Ref.[27]. However, for the composite coating, the surface oxide layer is uniform and compact, so further oxidation of the deeper layer is retarded, implying the oxidized surface is protective and the addition of amorphous Fe-based alloy do good to the thermal stability at 800 °C.

2.4 Electrochemical test

The potentiodynamic polarization curves of the two kinds of coatings in 3.5wt% NaCl solution are shown in Fig.11. The corresponding electrochemical values are listed in Table 2. It can be seen that the composite coating is spontaneously passivized with a passive current density in the order of magnitude about 10^{-4} A·cm^{-2}, while no obvious spontaneous passivation is observed in polarization curve of the WC-CoCr coating. The corrosion potential (E_{corr}) of the composite coating is –0.39 V, which is nobler than that of the WC-CoCr coating (–0.50 V). The corrosion current density (i_{corr}) of the composite coating is 3.25 μA/m^2, which is lower than that of the WC-CoCr coating (4.30 μA/m^2). Moreover, the polarization resistance (R_p) of the composite coating is 8006 Ω·cm^2, which is higher than that of the WC-CoCr coating (5962 Ω·cm^2). It is generally agreed that the extent of corrosion is determined by corrosion potential, polarization resistance corresponds to corrosion resistance, and besides the corrosion rate is proportional to the corrosion current density measured via polarization[28]. Therefore, the nobler E_{corr}, the lower i_{corr} and the higher R_p of the composite coating than those of the WC-CrCo coating indicates that the addition of FeCrMoWBMnCSi amorphous alloy in WC-CoCr coating improves the corrosion resistance in 3.5 wt% NaCl solution.

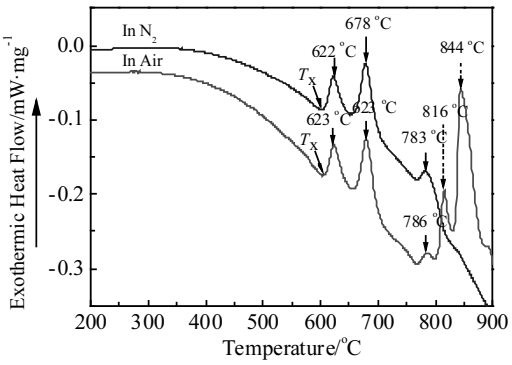

Fig.10 DSC curves of Fe-based amorphous powder tested in N_2 and in Air

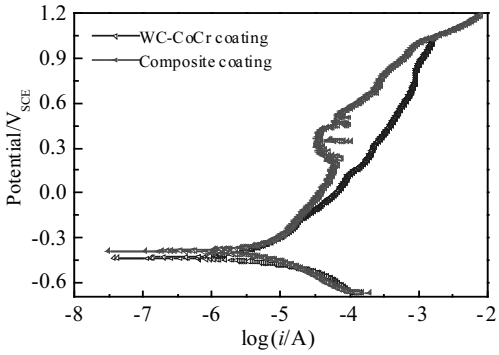

Fig.11 Potentiodynamic polarization curves of WC-CoCr coating and composite coating in 3.5 wt% NaCl solution

Table 2 Electrochemical values of the coatings

Coatings	E_{corr}/V	i_{corr}/μA·m^{-2}	R_p/Ω·cm^2
WC-CoCr	-0.50	4.30	5962
Composite	-0.39	3.25	8006

3 Conclusions

1) WC-10Co4Cr/Fe-based amorphous alloy composite coating has been deposited on 304 stainless steel by an HVOF spraying process.

2) The composite coating is mainly composed of WC, W_2C and Fe-based amorphous phase.

3) In comparison to a pure WC-CoCr coating, the thermal stability of the composite coating is enhanced by the for-

mation of a dense oxidized layer without any peeling off during high temperature oxidation test, and the corrosion resistance in 3.5% NaCl solution is improved, while the surface hardness and wear resistance of the composite coating are slightly decreased to different extents.

4) The composite coating with lower material cost exhibits excellent thermal stability and better corrosion resistance for wear application.

References

1 Agüero A, Camón F, De Blas J G *et al*. *Journal of Thermal Spray Technology*[J], 2011, 20(6): 1292

2 Fan Z, Wang S, and Zhang Z. *Rare Metal Materials and Engineering*[J], 2017, 46(4): 923 (in Chinese)

3 Pierre L, Fauchais J V R H, Boulos Maher I. *Thermal Spray Fundamentals. From Powder to Part*[M]. New York: Springer Science+Business Media, 2014

4 Thakura L, Arora N. *Journal of Materials Engineering and Performance*[J], 2013, 22(2): 574

5 Zhao L D, Maurer M, Fischer F *et al*. *Wear*[J], 2004, 257: 41

6 Li C J, Yang G J. *International Journal of Refractory Metals and Hard Materials*[J], 2013, 39: 2

7 Wu Y, Hong S, Zhang J *et al*. *International Journal of Refractory Metals and Hard Materials*[J], 2012, 32: 21

8 Yang G J, Gao P H, Li C X *et al*. *Scripta Materialis*[J], 2012, 66: 777

9 Yang G J, Gao P H, Li C X *et al*. *Applied Surface Science*[J], 2015, 332: 80

10 Ghadami F, Ghadami S, Abdollah-Pour H. *Vacuum*[J], 2013, 94: 64

11 Yang G J, Wang H T, Li C J *et al*. *Surface & Coating Technology*[J], 2011, 205: 5502

12 Richert M W. *Journal of Achievement in Materials and Manufacturing Engineering*[J], 2011, 47(2): 177

13 Zhang C, Liu L, Chan K C *et al*. *Intermetallics*[J], 2012, 29: 80

14 Wang S L, Cheng J C, Yi S H *et al*. *Transctions of Nonferrous Metals Society of China*[J], 2014, 24: 146

15 Qin Y J, Wu Y P, Zhang J F *et al*. *Transactions of Nonferrous Metals Society of China*[J], 2015, 25: 1144

16 Chokethawai K, McCartney D G, Shipway P H. *Journal of Alloys and Compounds*[J], 2009, 480: 351

17 Takeshi T, Fumiya T, Kazuhiro N *et al*. *Journal of Alloys and Compounds*[J], 2010, 504s: s288

18 Bolelli G, Börner T, Milanti A *et al*. *Surface and Coatings Technology*[J], 2014, 248: 104

19 Belashchenko V E. *Deposition System, Method and Materials for Composite Coatings*[P]. United States, 2007

20 Wang G, Xing C, Tao F *et al*. *Surface & Coating Technology*[J], 2016, 305: 62

21 Ding K, Guo Y, Cheng T *et al*. *Rare Metal Materials and Engineering*[J], 2017, 46(5): 1197 (in Chinese)

22 Tsotsos C, Yerokhin A L, Wilson A D *et al*. *Wear*[J], 2002, 253(9-10): 986

23 Ma H R, Li J W, Jiao J *et al*. *Materials Science and Technology*[J], 2017, 33(1): 65

24 Yugeswaran S, Kobayashi A, Suresh K *et al*. *Journal of Alloys and Compounds*[J], 2013, 551: 168

25 Yoon S, Kim J, Bae G *et al*. *Journal of Alloys and Compounds*[J], 2011, 509(2): 347

26 Meškinis Š, Puišo J, Juraitis A *et al*. *Materials Science (MEDŽIAGOTYRA)*[J], 2006, 12(3): 214

27 Mari D, Berger L M, Stahr S. *Solid State Phenomena*[J], 2012, 184: 313

28 Esmaeili M M, Mahmoodi M, Imani R. *International Journal of Applied Ceramic Technology*[J], 2017, 14(3): 374

铁基非晶合金增强碳化钨基涂层的结构和性能

徐丽萍，宋进兵，邓畅光，刘 敏，周克崧

（广东省现代表面工程技术重点实验室 现代材料表面工程技术国家工程实验室 广东省新材料研究所，广东 广州 510651）

摘 要：采用超音速火焰喷涂(HVDF)技术制备了 WC-CoCr/铁基非晶复合涂层。比较研究了复合涂层和 WC-CoCr 的微观形貌、硬度、耐磨性能、高温氧化性能和腐蚀性能。XRD 分析和 SEM 观察表明，复合涂层主要由 WC 相、W_2C 相和铁基非晶相组成。与 WC-CoCr 涂层相比，复合涂层的硬度有所降低，但是两者没有显著性差异。由于硬度下降，导致复合涂层的耐磨性能略低于 WC-CoCr 涂层。800 ℃高温氧化测试表明，复合涂层在 800 ℃具有良好的热稳定性，这归因于氧化过程中生成了一层致密的氧化膜。此外，复合涂层在 3.5%氯化钠溶液中的耐腐蚀性能也优于 WC-CoCr 涂层。

关键词：碳化钨基涂层；非晶；超音速火焰喷涂；耐磨性能；耐腐蚀性能

作者简介：徐丽萍，女，1977 年生，博士，高级工程师，广东省新材料研究所，广东 广州 510651，E-mail: xuliping@gdinm.com